DESCRIPTION OF EXPERIMENTS

1.7 THEORY

Limited testing of stiffened panels has been performed in the past because of the large loading demands involved. These demands present physical and economical issues that often limit the scope that testing may encompass. To perform full scale or half scale tests on specimens with multiple stiffeners, it was conceived to make the stiffened panel the tension flange of a box girder. This configuration maximized the stress that could be imparted on the stiffened panel with minimal loading. In four-point bending, the box girder test setup could achieve a constant moment region where fatigue activity could be monitored. The conceptual setup can be seen in Figure 0-1.

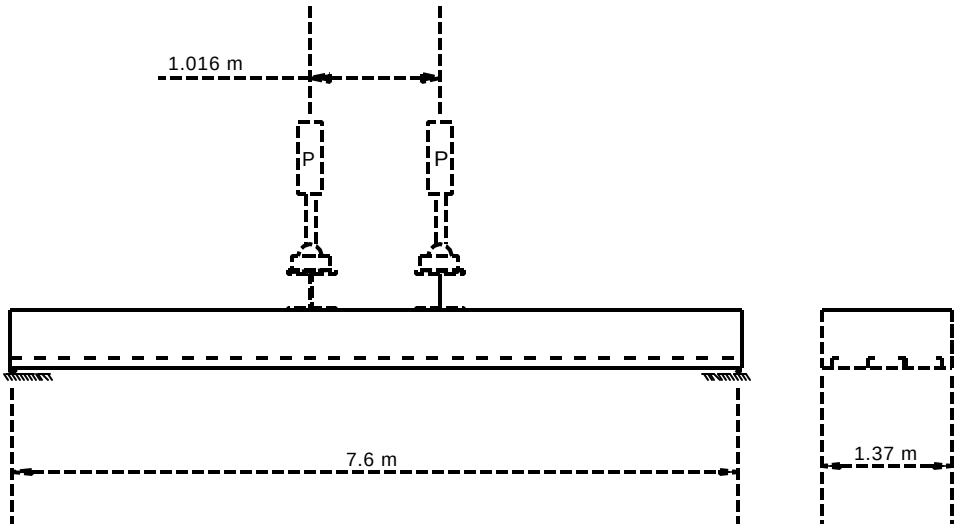

Figure 0-1: Initial conception of testing setup for fatigue experiments.

Financial constraints forced abandonment of monolithic test sections in favor of a bolt-up type specimen with standard W-shapes forming the superstructure. Bolted, slip-critical connections

transform the section from a pair of W12x72 beams at the supports to a large box girder at midspan. These modifications are shown in Figure 0-2.

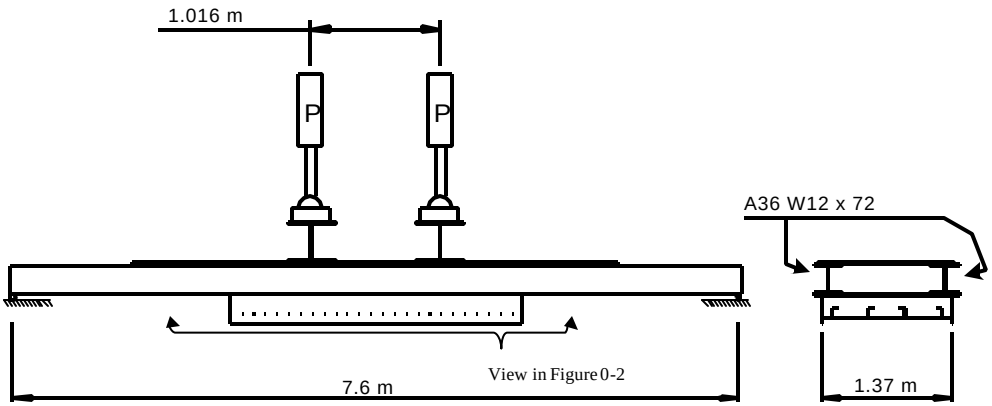

Figure 0-2: Revised experimentation setup after value engineering.

The overall length of the W12 x 72 support beams is 7.62 meters (25 ft) while the distance between supports is 7.112 meters (280 inches). Two 489 kN actuators provide the cyclic load at a distance of 1.016 meters (40 in) apart. A 19-mm thick cover plate spanned the width between the W12x72 beams, tying the beam compression flanges up to a distance 1.27 meters from the ends of the beams. The W12 x 72 beams were drilled with 120 holes matched to a template used for the specimens (Figure 0-3).

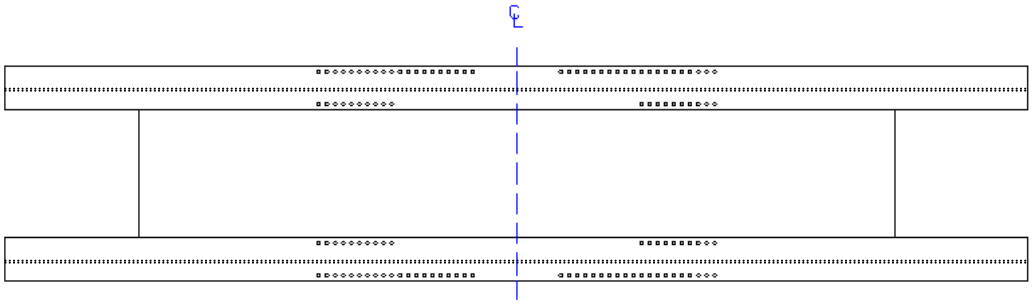

View of support structure from ground level

Figure 0-3: Hole pattern used for experiment assembly with 22-mm A490 bolts.

A490 bolts torqued to 949 N-meters (700 ft-lbs.) connect the top flange of the specimens to the bottom flanges of the W sections. The specimens were fabricated in 3.048-meter lengths, with typical panel widths of 1.37 meters and a plate thickness of 12.7-mm. Four stiffeners were mounted symmetrically in the stiffened panels at a spacing of 190.5-mm. Complete details of the composite cross section is shown in Figure 0-4 while Figure 0-5 illustrates a typical stiffened panel specimen.

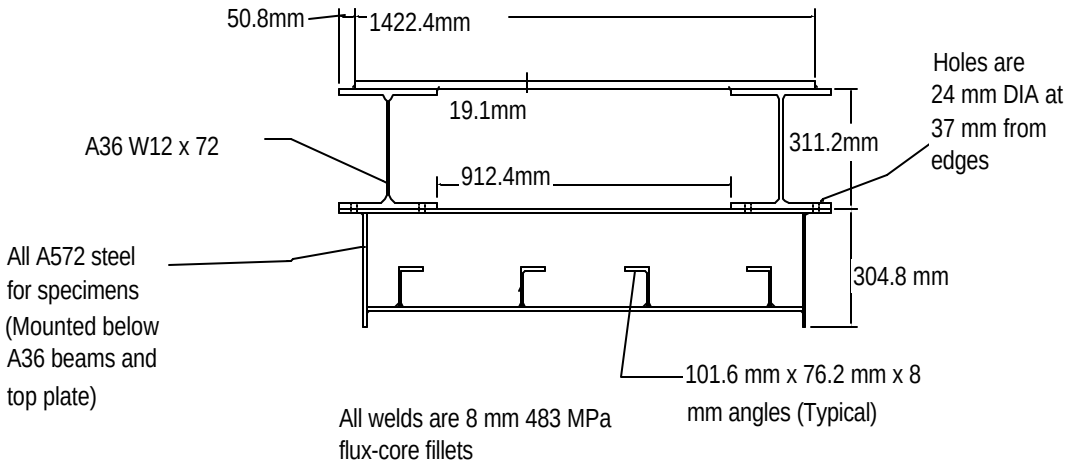

Figure 0-4: Cross section of support structure with specimen mounted below.

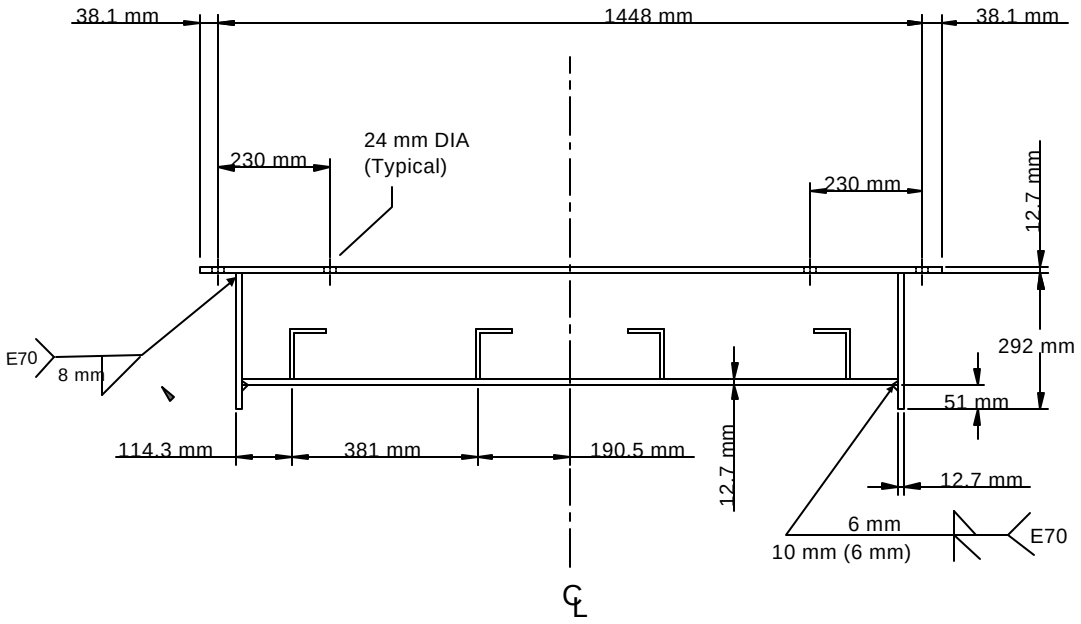

Figure 0-5: Typical stiffened panel specimen employed in experiments.

The total depth of the section is 63.5 cm, with the specimen depth equal to 30.5 cm. A scale of 2:1 was used in correlating specimen component dimensions with typical tanker structure. All of the stiffeners had unequal legs measuring 102 mm and 76 mm with an 8 mm thickness.

Initiation of testing with the baseline test section revealed applied stress ranges of 14 MPa in the stiffened panel, much less than the desired level. In order to raise the stress distribution in the panel and reduce the shear lag effects, vertical webs were fillet welded below the W12 x 72 beams in alignment with the webs of the specimens. Connecting these web additions to the specimens were 12.7 mm x 320-mm plates in a lap splice configuration. Eight A490 bolts were torqued to 949 Newton-meters to provide the slip critical connection. This connection improved the fatigue resistance of the added web at the fillet weld terminations by providing continuity between section changes. The web and splice plate additions can be seen in extending from the specimen (See Figure 3-6).

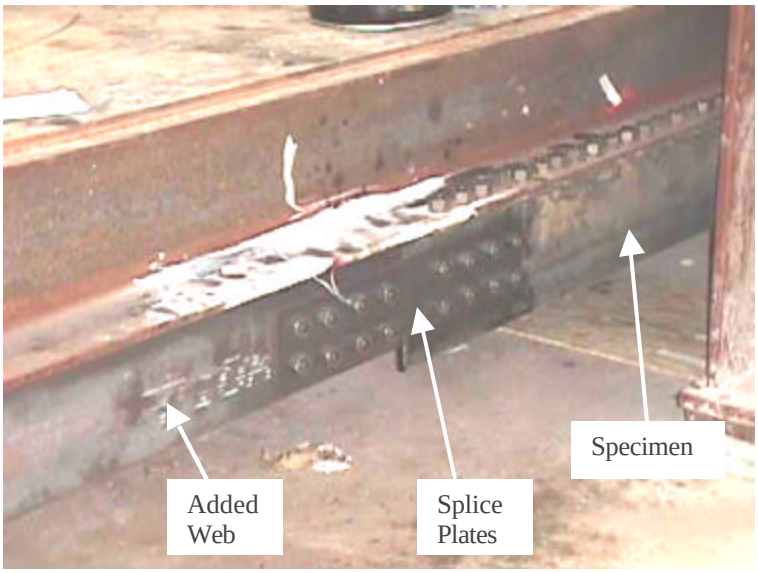

Figure 3-6: Splice plates bridging the gap between specimen and web mounted below W section.

With the splice plate addition, cyclic stress levels in the stiffened panel were increased to an average of 48 MPa. This applied stress range, although low, is very representative of the overwhelming majority of stress ranges seen in ocean vessels. The extreme wave loading for which ship structure is designed is a rare incidence if it ever is seen during a tanker's life. Consequently, most of the life of the ship undergoes cyclic stresses near the fatigue threshold of the material. The stress ranges in the experiments, therefore, will be a close resemblance of the actual sea state stresses.

However, a stress gradient was still experienced across the specimen width and in the stiffened plate. To monitor the experiments, strain gages were used at varying distances from the crack line. On the bottom plate, six strain gages were mounted 20 cm. from the crack line and an another three were mounted 76 cm. from the crack line. These strain gage locations can be seen in Figure 3-7.

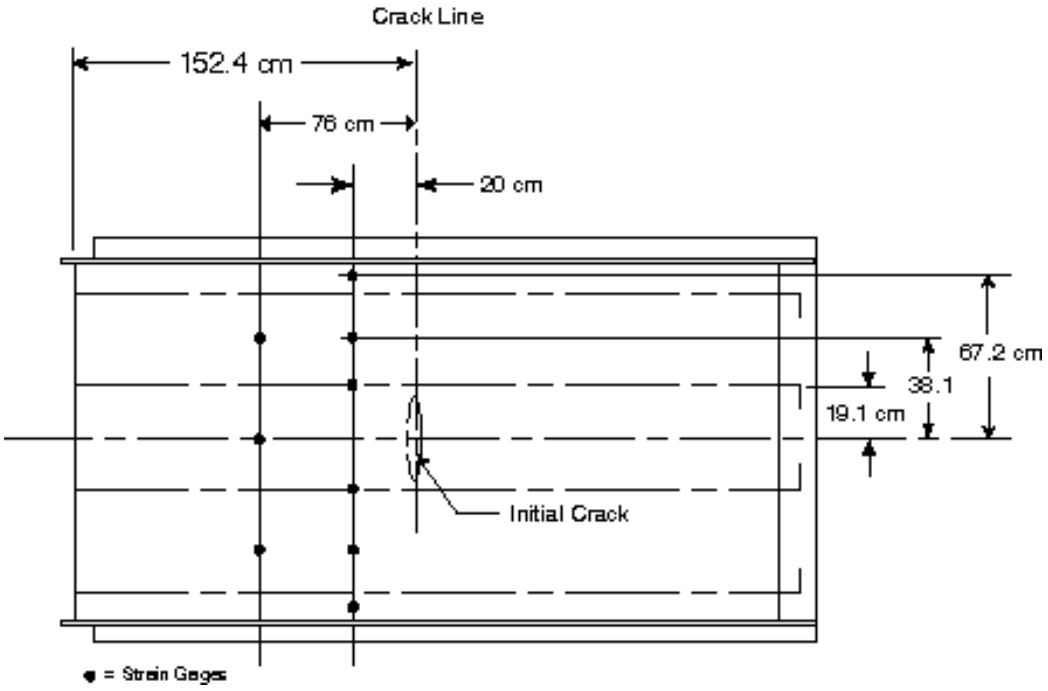

Figure 3-7: Strain gage locations on bottom plate used for stress range monitoring.

In addition, one strain gage was mounted atop the webs of an interior and an exterior stiffener for each specimen. The stiffener gages allowed observation of stress increases as the plate became cracked and shed load to the stiffeners. They also allowed an estimation of the number of cycles at which a crack would initiate in the stiffener details, i.e., a crack initiating at the top of a weld access hole.

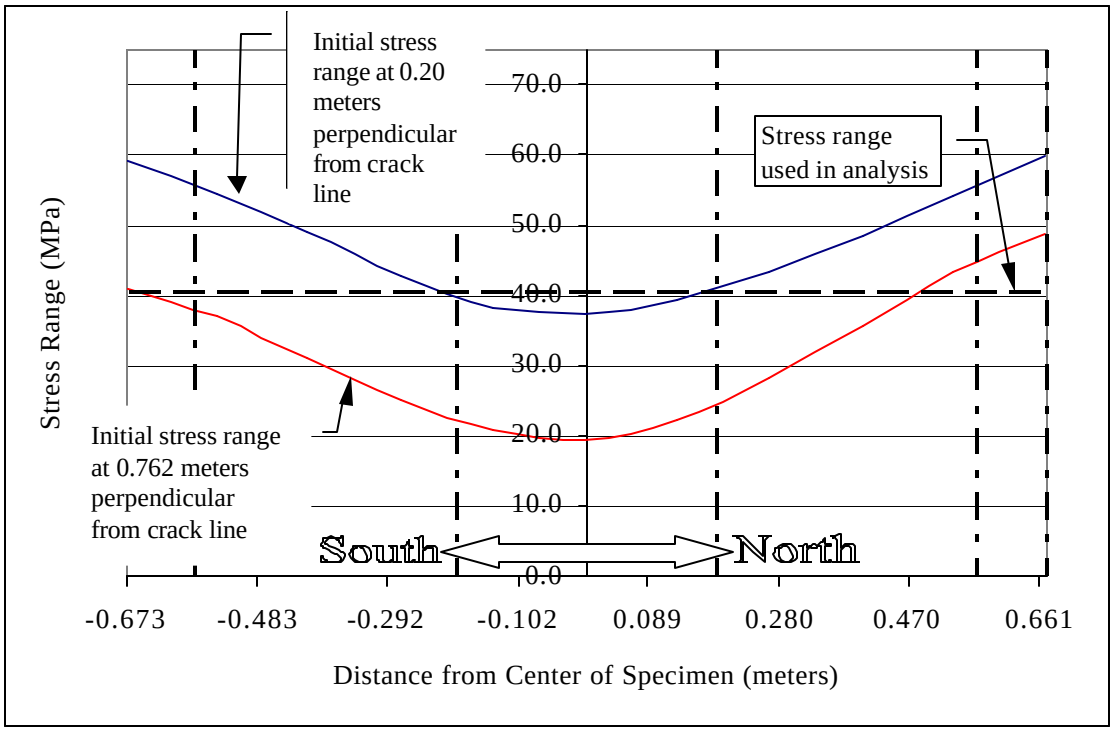

Figure 3-8: Stiffened plate stress gradient experienced in Case 2a (Typical of all cases).

Figure 3-8 illustrates the magnitude of the stress gradient and the gradual increase in stress as one nears the constant moment region. The four vertical centerlines denote the stiffener locations. The stress gradient curves were determined by fitting cubic splines through the strain data points.

The complete test setup allowed easy swapping of specimens, generous access for monitoring crack growth, and full recording of testing stress levels. Figure 3-9 shows a photo of the resulting test setup without a specimen mounted while Figure 3-10 shows a photo with the assembly complete.

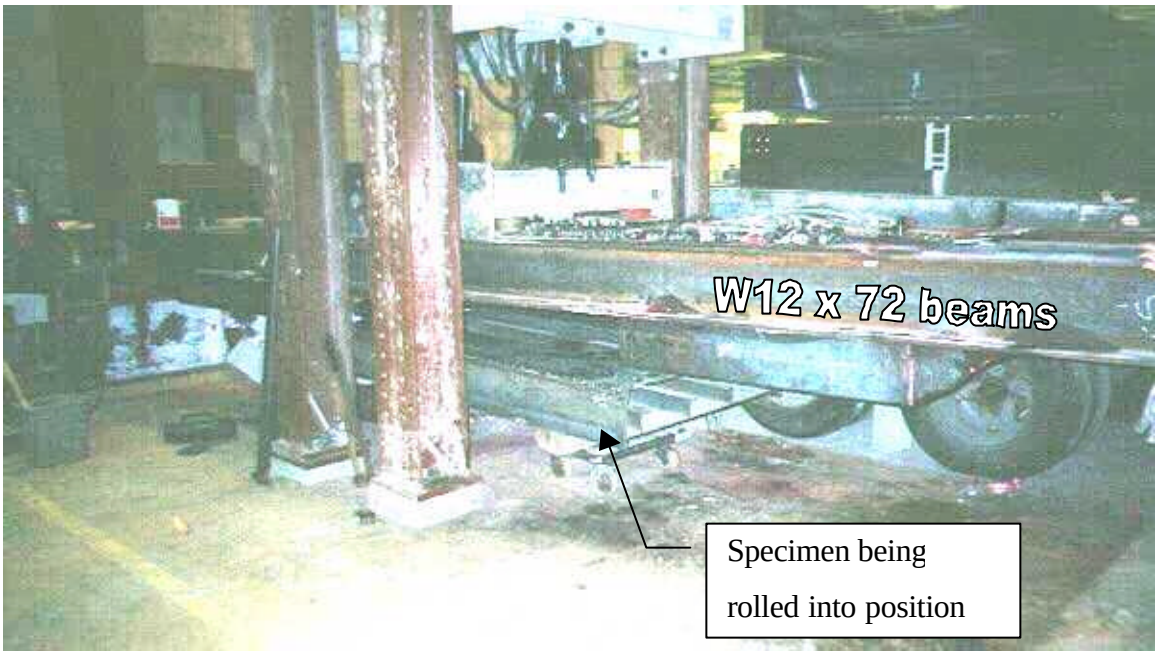

Figure 3-9: Test setup prior to assembly.

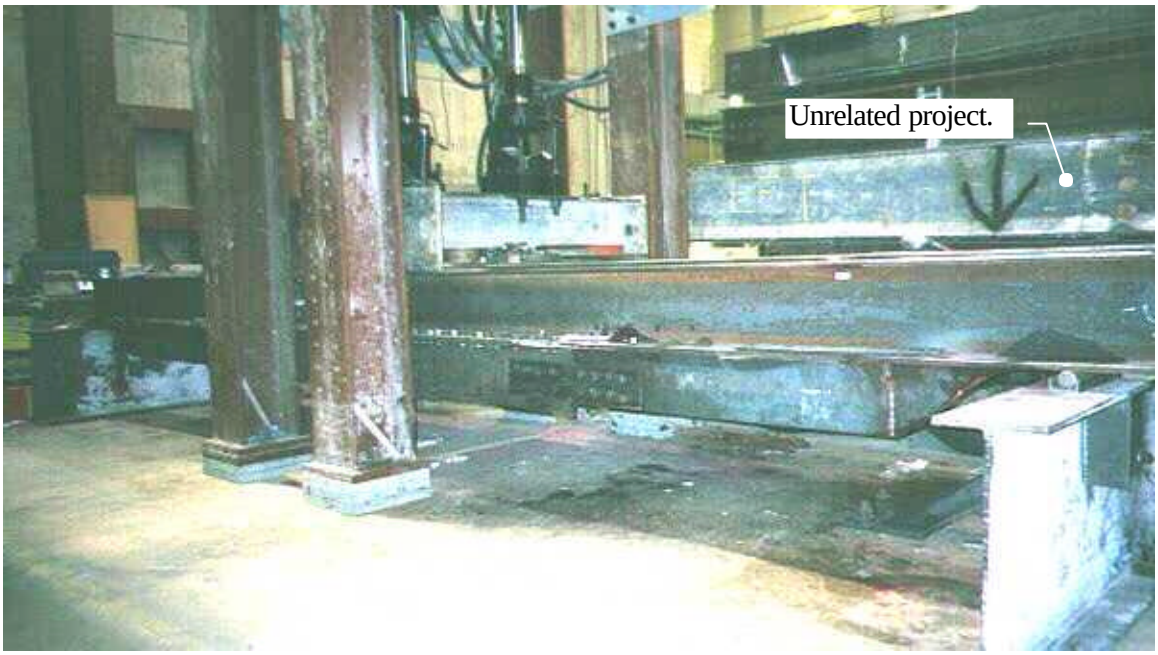

Figure 3-10: Test setup with assembly completed.

3.2 FABRICATION

The support structure and the specimens were fabricated at a local AISC certified fabricator, LeJeune Steel Company of Richfield, MN. The support structure material was A36 or A572, at the option of the fabricator. The chemical composition of the steel used to make the test specimens is listed in Table 3-1. The 13-mm plate was A572 steel while the angles were A588 steel, both have a minimum specified yield stress (MSYS) of 345 MPa.

Table 3-1 Chemical composition of steel used in specimens.

Element	Maximum percent by weight	
	A572 12.7 mm plate	A588 101.6mm x 76.2 mm x 8-mm angles (ASTM A709-50W)
Carbon	.05	.13
Manganese	.96	1.04
Phosphorous	.005	.018
Sulfur	.004	.04
Silicon	.03	.26
Copper	.08	.38
Nickel	.05	.17
Chromium	.04	.51
Molybdenum	.01	.048
Vanadium	.059	.044
Aluminum	.032	0
Niobium	.002	0

Higher-strength steel was chosen because it is though to represent typical ship steel better than steel with a MSYS less than 260 MPa. Table 3.2 shows the results of two flat-strap tensile coupons cut from the plate steel and one coupon cut from the angle sections. The tensile test data show that the strength is much higher than the MSYS. The strength level should not have a substantial effect on the fatigue behavior of the specimens. It is well known that the rate of crack propagation does not

depend on the strength level of the steel. If there is any effect, it is expected that the higher strength steel will exhibit greater effect of residual stress.

Table 3-2: Material strength properties.

	Yield Strength, MPa	Tensile Strength, MPa
Plate steel		
*Test 1	501.4	628.1
*Test 2	500.3	645.3
Angle steel	351.6	524.7

*replicate tests

(Note, to convert MPa to ksi, divide by 6.89)

All fillet welds were made using the FCAW process with an 8-mm weld size and 483 MPa wire (E70). Continuous double-sided fillet welds connected the stiffeners to the 12.7-mm thick bottom plate. These overmatched welds were used to maximize any effects of residual stress. A template was used for drilling the 120 holes in the specimen top flange in order to facilitate fit-up problems and minimize mechanical stresses.

3.3 SPECIMEN DETAILS

Cracking in ship structure often initiates at sources of stress discontinuity and abrupt changes in cross section, such as near hatch openings in the top deck. These discontinuities have been studied for years in order to achieve fatigue improvements and better performance. Nonetheless, fatigue cracks have become a frequent occurrence and the focus is shifted in this report to predicting fatigue crack propagation considering an initially cracked structure.

An existing, identified crack is easier to predict than a nonexistent one. The existing crack occupies a structural setting and has a generally known path--perpendicular to the principal

These facts allow one the benefit of knowing the environment, material, geometry, and loads in advance. The problem remains to simply identify the correct behavioral aspects of the crack under the corresponding conditions. This line of thought led to the development of several details identified as recurring environments for propagating fatigue cracks. The experimental setup does not consider the source of a crack; rather, it provides an ideal environment where specific geometries can be tested for their interaction effects on a running fatigue crack.

With this testing philosophy, the six specimens were designed to characterize common settings in ship structure. The first specimen, the baseline case, contained no stiffeners while five stiffened panels constituted the remainder of the testing schedule. Each of the five stiffened panels focuses on a specific type of detail and cracking scenario. Initially it was decided to start all fatigue testing of specimens, except for case 2, with an initial 200-mm notch sawcut in the specimen between the two interior stiffeners. This ideal, however, was soon deemed impractical as it was observed that peak loading conditions failed to propagate the crack with any marked progress. Therefore, initial sawcuts were incrementally lengthened in each specimen until a propagating crack was achieved in less than 300,000 cycles.

Case 1 consists of solid stiffeners with a 40 cm centrally cut notch. This case will attempt to define crack-stiffener interaction in situations where an existing crack intersects a solid stiffener.

Cases 2 and 2a are identically built with 51-mm diameter weld access holes (rat holes) at the centerline of each stiffener. These weld access holes are required at discontinuities in hull plating. Case differences arise in the initially introduced cracks in cases 2 and 2a. The initial notch in case 2a is a 28-cm sawcut centrally located between the interior stiffeners, while case 2 contains short initial notches located at the fillet weld terminations in the weld access holes.

Case 3 incorporates a flame cut raised drain hole at the centerline, a slotted hole (37-mm x 19-mm). The specimen contained a 30-cm initial notch located between the interior stiffeners.

Case 4 contains a transverse butt weld with weld access holes (rat holes) in the stiffeners. This specimen attempts to simulate the master butt weld in ship construction, where two cross sections of ship hull are butted together and welded with a complete penetration butt weld. An initial crack 20-cm in length was saw cut into the specimen 4 between the interior stiffeners.

These different details are shown in Figure 3-11. An illustration of these details in ship structure can be seen in Figure 0-12.

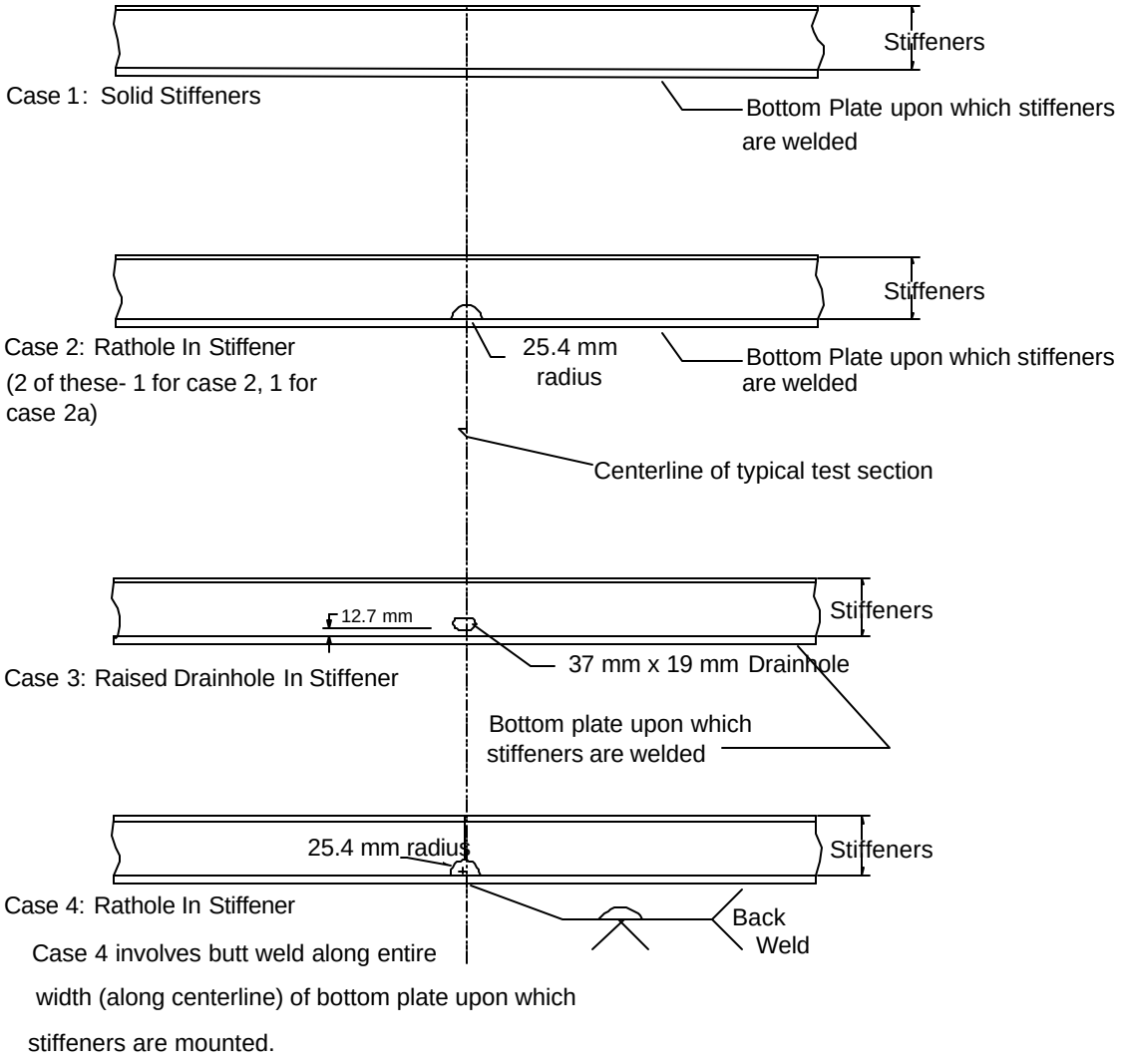

Figure 3-11: Various details tested in experiments.

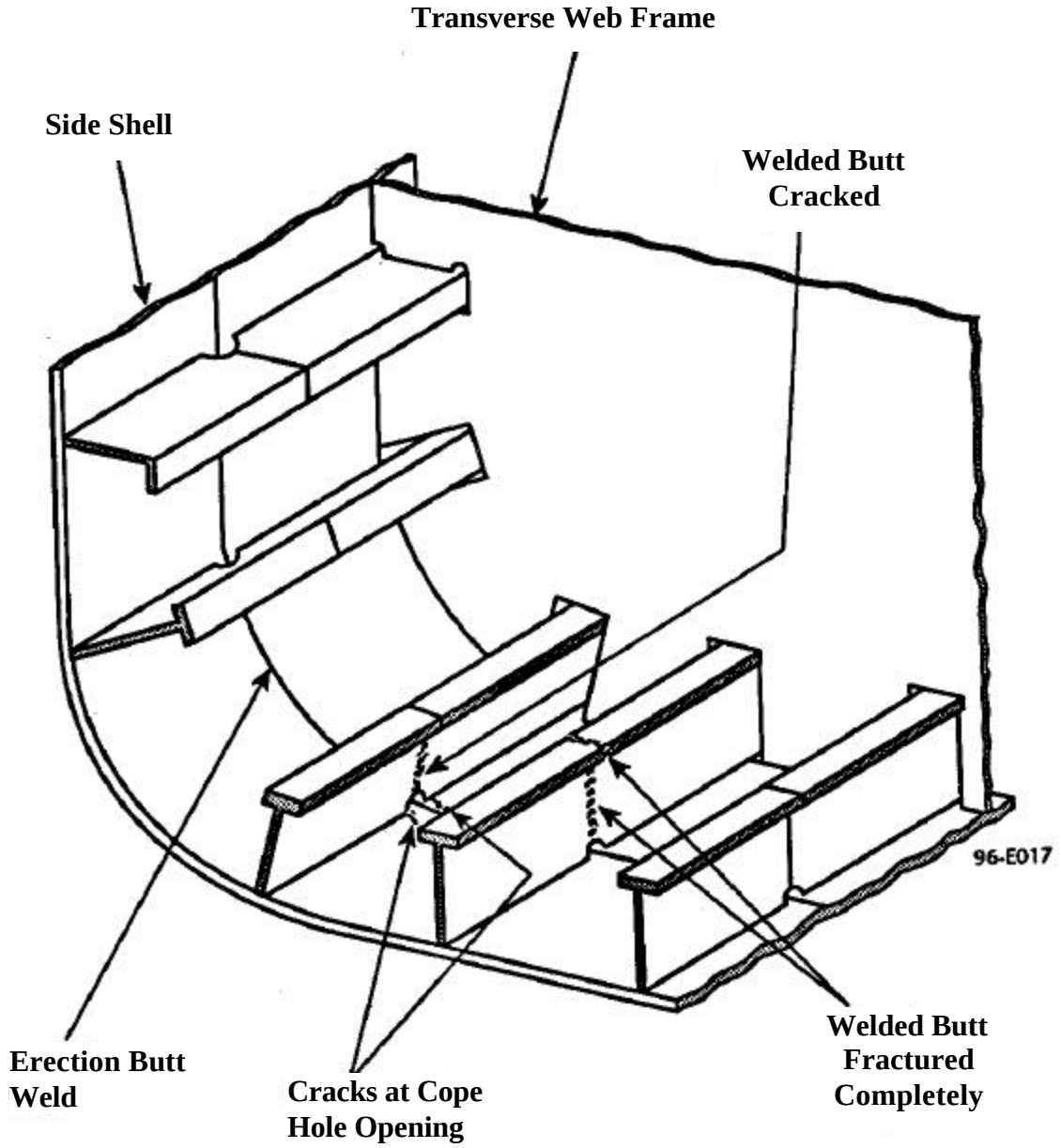

Figure 0-12: Typical fatigue sensitive details in ship structure [35].

Case 4 can be seen in Figure 3-13 prior to installation under the support structure. A large opening was cut into the top flanges of the specimens after testing of the baseline case and case 2a because

limited load shedding and negligible displacements were observed with crack growth. The opening also allowed greater access to the interior for crack growth monitoring in the stiffeners.

Figure 3-13: Case 4 with viewport cut into middle flange prior to testing.

Prior to installation under the support structure, the initial crack was cut into the specimens. This initial cut was made by first drilling an access hole for the reciprocating blade and then using the reciprocating saw to cut up to the desired length. At the end of the introduced crack, the saw-cut was beveled through the thickness at a 30-degree angle in order to facilitate the formation of a crack. This initial cut can be seen in Figure 3-14.

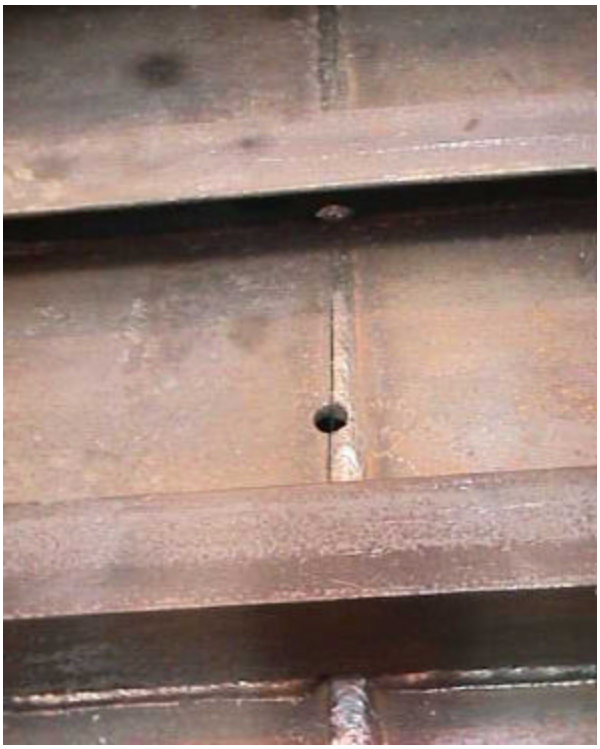

Figure 3-14: Typical initial crack introduced in specimen with reciprocating saw.

3.4 TESTING PARAMETERS

Ship structure and many other structurally redundant systems exhibit a mixture of load control and displacement control. Load control occurs when the applied loads do not diminish in response to increased compliance in a system. For example, a ship exposed to wave loading has a constant, repeated load applied to it. A reduction in net section will make the structure increase its displacement response, but the applied loading does not diminish. This is the case when a crack forms and releases any forces previously carried by the cracked area, effectively transferring its load to adjacent structural components. This effect is appropriately termed load shedding.

Load shedding contributes to another identifiable structural behavior on a local scale, called displacement control. Displacement control is seen when a crack is limited in the degree it may open by adjacent structural members. The adjacent members simply become more stressed while

restraining the local separation. Structurally redundant ships exhibit a great deal of displacement controlled behavior due to numerous load paths inherent in the cellular structure. These definitions illustrate the complimentary relationship between displacement control and load control that is linked through load shedding. This relationship is very difficult to quantify in a general sense, and thus a conservative approach should assume a load-controlled state. When adjacent redundant members are capable of handling the load from the cracked section without severe deformation, it would be acceptable to assume displacement-controlled loading.

Ideally, a variety of testing conditions would be addressed in each specimen configuration. In this testing program, however, the effect of local stiffener geometry was addressed. All of the specimens were tested under the same conditions to single out the effects of the different stiffener details. In fact, many variables were not changed, or altered only slightly, during the experimentation. These include:

- Temperature
- Load ratio
- Material
- Stiffener size
- Weld metal and size
- Weld process
- Testing frequency
- Environmental effects

In the experimental study, the variable of temperature is held constant at the temperature of the laboratory. Temperature may play a significant role in the global stresses that a region in ship structure may experience. Temperature variance between the interior of a ship hull and exterior hull has induced large stresses responsible for crack initiation at susceptible details [6].

Once a crack has developed, temperature effects in ship structure become negligible. There are several reasons for this. First of all, the main parameters for fatigue crack propagation are the applied stress range and number of cycles. Since a temperature loading is far less frequent than a wave loading, its contribution to the fatigue crack propagation may be ignored. Secondly, the temperature of the salt water does not drop below its freezing point in a sea environment. The temperature of the steel hull matches that of the water it is in

contact with. In other regions of the ship, such as the deck plating, the temperature may be significantly lower in a frigid environment. In these regions the crack propagation rate would increase slightly. Once again, however, the temperature effects are negligible compared to the effects of applied stress and number of cycles, and can be conservatively accounted for by increasing the coefficient *C* in the Paris Law.

The load ratio has been discussed in the introduction to fracture mechanics, Chapter 2. A load ratio of 0.15 or less is used throughout the experiments. At no point during the testing schedule is a portion of the loading cycle compressive. This has been done to isolate the effects of residual stress on crack growth rate.

All specimens were constructed of the same materials as described earlier in this chapter. Crack propagation rates are virtually identical in most types of steel. This fact is directly seen in the exponent, *m*, of the Paris Law, which has a value of three for steel. Furthermore, the material toughness was not considered or even accounted for in the testing. Toughness was neglected because minimum material toughness levels have existed for several decades in ship construction. These minimum levels assure ductile fracture, and hence stable crack growth, under uniaxial applied stresses. In other words, as long as minimum toughness levels exist in the material the behavior of fatigue crack propagation will not be marked by sudden fracture. As the net section is reduced by fatigue crack propagation, however, a net section fracture based on the ultimate tensile strength of the material can be expected.

Stiffener size was not varied in this project. The stiffeners are approximately ½ scale of full size longitudinals in TAPS trade tankers. Unequal angles having a 101-mm web, a 76-mm flange and a uniform thickness of 9-mm were employed. The stiffener details and their effects on crack propagation were the primary concern in the testing. For this reason, the stiffener size was held constant while the cutouts and local discontinuities were varied. Also, the number of stiffeners in the panel was limited to the physical width of the testing structure and the scaled stiffener spacing. In this regard, four stiffeners were used in each specimen in a symmetric configuration.

Various welding practices and processes are employed in ship construction. To thoroughly test each process in combination with different sequencing methods would be excessive. Instead, the approach taken in this project is to determine worst case crack growth rates and magnify the effects of residual stress due to welding. With this philosophy, oversized welds were used in assembling the specimens to magnify any residual stress patterns. The welds were all made with E70 wire in a flux-core arc welding (FCAW) process.

Construction sequencing is responsible for mechanical residual stress, or internal stresses that result from improper fit and assembly distortion. There is an intimate relationship between welding-induced residual stress and mechanical residual stress, the latter often being affected by welding distortion. For example, the fabrication of the specimens involved welding the stiffeners to the bottom plate before the top plate and side webs were added. Once the stiffeners were mounted, the side webs were attached. This sequence made the webs "bow out" initially, a reaction to the thermal cooling of the web–bottom plate welds. The web bow was forced into the desired position on the top plate prior to its assembly. This induced mechanical stresses in the specimens.

Special attention was given to specimen four. This specimen incorporated a butt weld typical of the junction of two ship sections, usually termed an erection butt weld. An example of such a joint is shown in Figure 0-12. In order to capture the residual stresses in such a junction, the stiffeners were welded to two separate bottom plates first. The stiffeners themselves were not spliced. Next, the two bottom plates were attached with a full-penetration groove weld, followed by the joining of the side webs and top plate. This sequence attempts to simulate the mechanical and thermal residual stresses resulting from the connection of two ship sections or, alternatively, a weld repair made in a previously cracked section. Constraint from attached stiffeners to the two bottom plates creates large tensile residual stresses in the butt weld region, which can magnify the fatigue crack propagation rate.

Another variable involved in fatigue crack propagation is the cycling frequency. The experiments were conducted with a frequency of 1.2 Hertz. Usually a higher cycling frequency translates to an increased fatigue crack growth rate because the strain rate is increased. An increased strain rate affects crack growth only marginally unless the increase is of several magnitudes. Wave loading in ship structures is stochastic in nature and may be assessed with frequencies less than 2 Hz. However, slamming loading, i.e. the effect of waves impacting a portion of the hull from the side, can dramatically increase fatigue crack propagation. This type of loading was not investigated in this report.

The frequency effects in ship structure may be tied to environmental effects. A salt-water environment induces corrosion in exposed metal. The primary effect of the corrosion is to thin the plating, leading to an increase in the stress ranges. Other than this effect, corrosion has mixed effects on the crack propagation. At high growth rates, the effect of corrosion essentially doubles the rate of crack growth at a specific level of ΔK. However, corrosion also substantially increases the threshold for fatigue crack growth, an effect which is beneficial! These two effects tend to cancel themselves out in the total effect on fatigue life for realistic variable amplitude loading histories comprised primarily of small stress ranges. Therefore, neglecting the corrosive environment is appropriate. For this reason and because of the testing complexities, the environmental effects were ignored in the experiments.

The actuators were run in load control. This type of testing incorporates the net section reduction and the associated increase in the applied stresses caused by cracking. The bolt-up design of the experiment, however, was found to have inadequate connection rigidity to exhibit continuous section behavior. In other words, the stress at a point in the composite cross section could not be predicted using simple flexure theory. To determine the stress distribution through the cross section a number of strain gages were placed along the depth of the section. The results, shown in Figure 3-15, illustrate the lack of bond between the specimen and the support structure.

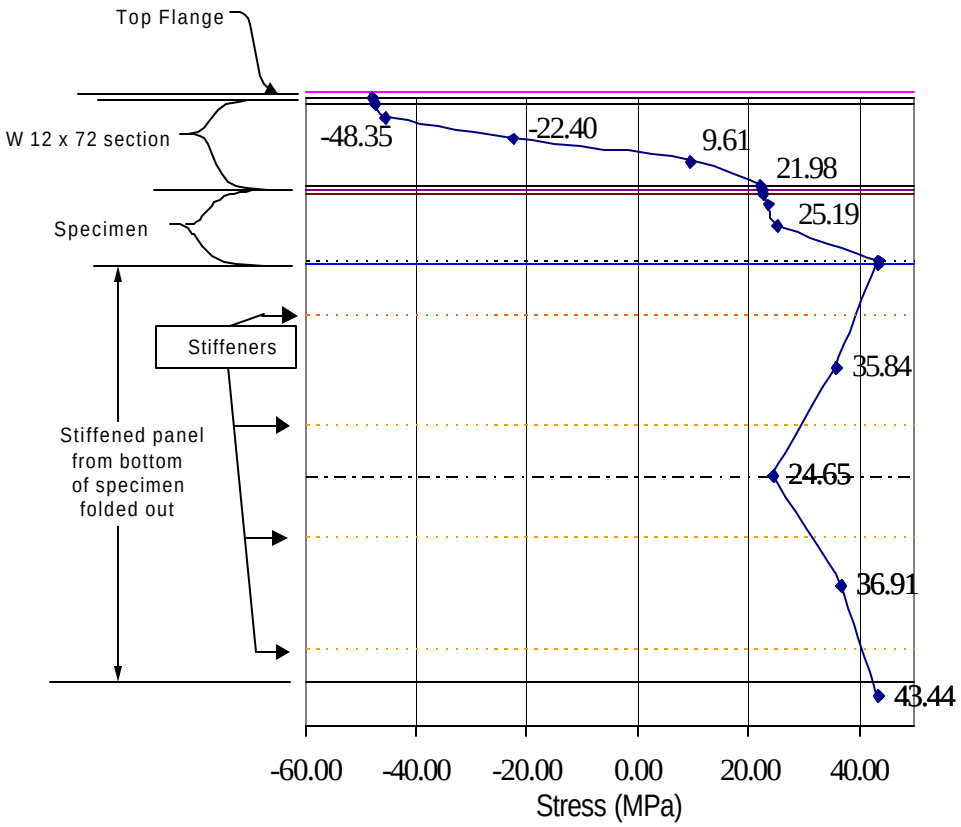

Figure 3-15: Stress gradient experienced in Case 2a (Typical of all cases).

From this investigation it was apparent that the experimentation would be performed at a compromise between displacement-controlled testing and load-controlled testing. The drawback of this situation is that most prediction methods are based on either an applied load analysis or an applied displacement analysis. Since the testing could be classified as neither loading condition completely, it was decided that intermittent stress readings be taken throughout the testing. Such data would assure accurate information would be available for developing prediction models. These stress readings were taken at the points shown in Figure 3-7.